Polymer Chemistry

Accepted Manuscript

ROYAL SOCIETY OF CHEMISTRY

www.rsc.org/polymers

Polymer Chemistry

ARTICLE

Synthesis and properties of polyesters derived from renewable eugenol and α,ω-diols via a continuous overheating method

Received 00th January 20xx,
Accepted 00th January 20xx

DOI: 10.1039/x0xx00000x

www.rsc.org/

Keling Hu,[a] Dongping Zhao,[a] Guolin Wu*,[a] and Jianbiao Ma*,[b]

Two eugenol-based aromatic dimethyl terephthalate (DMT)-like monomers were prepared via thiol-ene click reaction and subsequent nucleophilic substitution reactions with methyl chloroacetate or 1,4-dibromobutane. Two series of thermoplastic polyesters derived from renewable eugenol and linear aliphatic α,ω-diols HO-$(CH_2)_n$-OH (n = 2, 3, 4, 6, 10, 12) were successfully synthesized. These prepared polyesters have weight-average molecular weights in the range of 18500-90500 g mol^{-1}, and polydispersities (PDI) between 1.8 and 2.2. Their chemical structures were all accurately characterized by ^{1}H NMR, ^{13}C NMR and FTIR. The random microstructures of synthetic polyesters were also explored by ^{13}C NMR. The obtained polyesters all exhibit thermal stability above 330°C. More importantly, the thermal stability, the maximum degradation rate and residue weight are intimately associated with the length of the linear aliphatic α,ω-diol. Their thermo-mechanical properties were studied by the differential scanning calorimetry (DSC) and dynamic mechanical analysis (DMA). The length of linear aliphatic α,ω-diol shows crucial influence on the glass transition temperature (T_g). With the gradually increase of the α,ω-diol length, the T_g of the synthesized polyester uniformly exhibits a tendency of decreasing. The polyesters are all amorphous materials at room temperature, whose T_g values range from -28.4 to 7.6°C. The incorporation of aromatic eugenol into the polyester chains reduces the crystallinity obviously, as well as the mechanical properties compared with conventional PET or PBT. The Young's modulus and ultimate strength are just in the range of 1.2-6.9 MPa and 0.96-3.37 MPa, respectively. On the contrary, the elongation at break reaches up to 840-1000%, indicating the excellent viscosity properties for such unmanageable viscous materials.

Introduction

Poly(alkylene terephthalate)s, in particular, PET and PBT, are materials with widely applications and irreplaceability in the thermoplastic field. However, almost all of these plastics are produced from fossil resources at present. The temporary huge consumptions of these requisites need to look for renewable substituents urgently wherever or whenever to replace the exhausting petroleum-based resources.[1-4] The quantity of plastics produced currently in the world is around 250 Mtons per year with an average annual growth rate of 10%.[5] Almost half of the plastics serve as short-term packaging materials, beverage bottles or absorbable sutures.[6] Simultaneously, such huge consumptions bring inevitable environmental pollutions. The continuous consumption of petrochemical feedstock and deteriorating environment in turn cause the price fluctuations of fossil resources.[7] In brief, urgent actions are necessitated to make plastics renewable via using naturally-occurring raw materials and to take advantage of the synthetic potential of nature. Moreover, novel technologies and greener synthetic routes are required to be exploited in order to make the plastics degradable and recyclable.[8-13]

The most widely used renewable raw materials for non-fuel applications in chemical industry embrace plant oils,[14-16] lignin,[17] polysaccharides (mainly cellulose and starch),[18] sugars,[19] suberin,[20] cutin,[21] furfural[22] and others.[23-26] Plant oils stand out as the most appealing feedstock affording surfactants,[27] lubricants[28] and cosmetic products[29] by the route of chemical synthesis in the last two decades. By means of simple chemical reactions, fatty compounds are available from vegetable oils to get the purity that they can be used for further chemical conversions and for the synthesis of chemically pure monomers. Primarily, oleic acid, elaidic acid, linoleic acid, linolenic acid, erucic acid and ricinoleic acid have been used in the synthesis of bio-based linear or cross-linked polymers (*e.g.* polyolefins,[30] polyesters,[31] polyethers,[32] polyamides,[33] epoxy[34] and polyurethane resins,[35] and others[36]). Ricinoleic acid contains an appended secondary hydroxyl group which is productive in stereo and regioselective synthesis.[15] By pyrolysis of ricinoleic acid and subsequent hydrolysis, 10-undecenoic acid, a ω-unsaturated carboxylic acid, is obtained which is very useful for selective reactions and click reactions.[37] In our previous report, vanillic acid-based polyesters were prepared combining with thiol-ene coupling

[a] *Key Laboratory of Functional Polymer Materials, Institute of Polymer Chemistry, Nankai University, Tianjin 300071, P R China.*
[b] *School of Chemistry and Chemical Engineering, Tianjin University of Technology, Tianjin 300191, P R China*
† Electronic Supplementary Information (ESI) available: [Additional figures]. See DOI: 10.1039/x0xx00000x

reactions of 10-undecenoic acid, which have comparative thermal stability and mechanical properties with conventional polyester materials.[38]

Eugenol, another abundant plant component of lignin except for vanillin, exists naturally in the dried flower bud of clove that is rich in clove oil.[39] By means of simple distillation, extraction and neutralization, the eugenol product can be obtained from naturally-occurring raw materials. Regarding industrial synthesis method,[40] the petroleum-based *o*-methoxyphenol firstly reacted with allyl bromide to obtain the *o*-methoxyphenyl allyl ether, which was subsequently suffered from one-step Claisen rearrangement, the desired product eugenol was obtained. However, it is difficult to obtain high-purity product via this method because the products contain isomerides with close boiling points. Therefore, the eugenol product is generally obtained by extracting from clove oil. Accompanied by the huge consumption of plastics (*e.g*. PET and PBT) and the depletion of fossil resources, it is urgent to seek renewable substituents of dimethyl terephthalate (DMT) without compromise of thermal stability and mechanical strength. Eugenol, as a renewable aromatic monomer, emerges appropriately to solve the puzzle timely and has the potential to replace the petroleum-based monomers, which are currently widely used in the field of polyesters.

In this work, two aromatic DMT-like monomers derived from eugenol were prepared via thiol-ene click reaction[41, 42] and subsequent Williamson ether synthesis.[43] Firstly, the terminal olefinic bond of eugenol clicked with methyl thioglycolate to afford the precursor **P1**. Subsequently, the precursor **P1** reacted with methyl chloroacetate to afford the unsymmetrical diester monomer **M1**. In order to evaluate the impact on the properties (thermal and mechanical), 1,4-dibromobutane bridged symmetrical monomer **M2** was also prepared via Williamson ether synthesis. In order to compare the properties (*e.g*. glass transition temperature (T_g), crystallizability, thermal and mechanical) of polyesters derived from eugenol with conventional PET and PBT, two series of polyesters based on **M1** and **M2** were prepared with linear aliphatic α,ω-diols HO-$(CH_2)_n$-OH (n = 2, 3, 4, 6, 10, 12) via a continuous overheating method. That is, under the premise that the transesterification reactions proceed efficiently, the selection of transesterification temperature should be as low as possible in order to diminish the loss of α,ω-diols as much as possible and transesterification temperature are successively raised accompanying with the increase of viscosity. Moreover, special attention was paid to the influence of α,ω-diol length on the properties of the synthesized polyesters.

Experimental section

Materials

Eugenol (99%), methyl thioglycolate (99%), methyl chloroacetate (98%), 2,2-dimethoxy-2-phenylacetophenone (DMPA, 99%) and tetrabutyl titanate (TBT) (≥99%) were purchased from Sigma-Aldrich. Ethylene glycol, 1,3-propanediol, 1,4-butanediol, 1,6-hexanediol, 1,10-decanediol and 1,12-dodecanediol were obtained from Shanghai Aladdin Chemical Reagent Co. 1,4-dibromobutane (98%) and other common used chemical reagents were purchased from Tianjin Chemical Reagent Co. (Tianjin, China) and used without further purification. Acetonitrile and other solvents were dried according to the standard methods in the literature if necessary.

General instrumentation and method

^{1}H NMR and ^{13}C NMR spectra were recorded in $CDCl_3$ using a Bruker AVANCE III 400MHz NMR spectrometer at room temperature. Tetramethylsilane was used as the internal standard. Fourier transform infrared spectra (FTIR) were measured using a Bio-Rad FTS6000 spectrophotometer at room temperature. Polymer samples were prepared by adequately grinding the polymers with KBr powder and compressing the mixtures to form a disk. Fourier transform high resolution mass spectra (FTMS) were measured on the Varian 7.0T FTMS with an electrospray ionization (ESI). The molecular weights and polydispersities of polymers were determined through size exclusion chromatography (SEC, Waters 1525 dual pump, Waters 2414 differential refraction detector, Waters 2487 dual UV detector and Waters 717 plus automatic sampler) at 35°C. THF was used as the eluent at a flow rate of 1.0 mL min^{-1}. The average weights were calibrated with standard polystyrene samples. Thermogravimetric analysis (TGA) was performed on the NETZSCH TG209. Polymer samples were heated from 25 to 600°C at a rate of 10°C min^{-1} under a nitrogen atmosphere. Temperature leading to 5% weight loss and temperature for maximum degradation rate were acquired. Differential scanning calorimetry (DSC) thermograms were measured using a DSC Q100 apparatus from TA instruments. Polymer samples were first heated from 25 to 150°C and then cooled to -80°C. The T_g were calculated from the second heating run. All runs were performed at a rate of 10°C min^{-1}. The tensile assays were performed in triplicate on dog-shaped sample bars (12 mm × 2 mm × 0.5 mm) at 25°C and a rate of 50 mm min^{-1}. Young's modulus, tensile stress at break and tensile strain at break were acquired by averaging the data from the three paralleled test specimens. Dynamic mechanical analysis (DMA) were studied using a NETZSCH DMA242 in the controlled force-tension film mode with a preload force of 0.1 N, an amplitude of 10 mm, and at a fixed frequency of 1 Hz in the -60 to 60°C range and at a heating rate of 3°C min^{-1}. All the films with a thickness of about 0.5 mm used for tensile tests and DMA were obtained by casting from a chloroform solution at a concentration of 0.1 g mL^{-1}.

Synthesis procedures of precursor P1 and monomers M1, M2

Preparation of precursor P1: 2-methoxy-4-[3-(2-methoxy-2-oxoethyl)]thiopropyl phenol. Eugenol (6.62 g, 40 mmol), methyl thioglycolate (5.14g, 48 mmol), and 2,2-dimethoxy-2-phenylacetophenone (DMPA, 0.0514 g, 0.2 mmol) as the photoinitiator, were transferred into a 25 mL quartz tube and adequately mixed into a homogeneous phase (Scheme 1). Then the reaction system was irradiated with four 6W ultraviolet lamps (λ = 365 nm). The reaction was detected by TLC (thin-layer chromatography) until eugenol completely

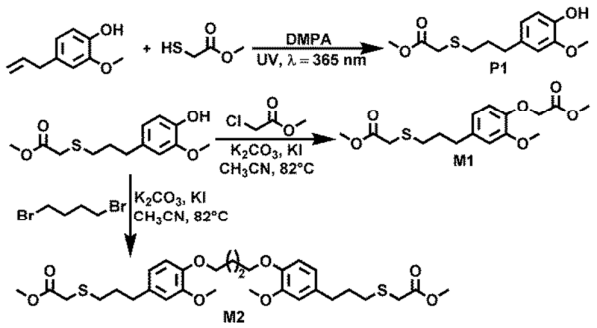

Scheme 1 synthetic routes of bio-based precursors **P1** and monomers **M1**, **M2**.

disappearing. The crude product was immediately purified by column chromatography (PE : EA = 5 : 1) to afford 10.24 g **P1** as a yellow oil. 95% yield; b.p.183-185°C (5 mmHg).

^{1}H NMR ($CDCl_3$, 400 MHz): δ 1.85-1.93 (quint, *J* = 7.3 Hz, 2H, -SCH_2-CH_2-), 2.61-2.66 (m, 4H, -S-CH_2-CH_2-CH_2-), 3.22 (s, 2H, -S-CH_2-$COOCH_3$), 3.71 (s, 3H, -CH_2COO-CH_3), 3.86 (s, 3H, ArO-CH_3), 5.53 (s, 1H, Ar-O*H*), 6.65–6.83 (m, 3H, Ar-*H*) ppm; ^{13}C-NMR ($CDCl_3$, 100.6 MHz): δ 30.79 (-SCH_2-CH_2-), 32.05 (-S-CH_2-CH_2-), 33.43 (Ar-CH_2-), 34.27 (-S-CH_2-$COOCH_3$), 52.32(-COO-CH_3), 55.92 (ArO-CH_3), 111.28 (Ar-*C*), 114.46 (Ar-*C*), 121.03 (Ar-*C*), 133.20 (Ar-*C*), 143.94 (Ar-*C*), 146.61 (Ar-*C*), 171.07 (-SCH_2-*C*O-OCH_3) ppm; HRMS (ESI) m/z calcd for $C_{13}H_{17}O_4S$ $[M-H]^-$: 269.0848, found 269.0852.

Preparation of monomer M1: methyl 2-{2-methoxy-4-[3-(2-methoxy-2-oxoethyl)]thiopropyl}phenoxy acetate. Precursor **P1** (5.40 g, 20 mmol), methyl chloroacetate (5.32 g, 40 mmol), anhydrous K_2CO_3 (5.52 g, 40 mmol), KI (0.166 g, 1 mmol), and 100 mL anhydrous CH_3CN were added into a 250 mL three-necked round bottom flask equipped with a magneton (Scheme 1). Subsequently, the reaction mixture was refluxed at 82°C for 6 h in the protection of nitrogen. Then the suspension was cooled to room temperature, white solid was filtered off. The filtrate was concentrated under vacuum. The residue viscous oil was redissolved in 200 mL dichloromethane and successively washed by water (2 × 60 mL) and saturated NaCl solution (2 × 60 mL). The organic phase was dried over anhydrous magnesium sulphate, concentrated under vacuum. The resulting residue was purified by column chromatography (PE : EA = 3 : 1) to afford 5.92 g **M1** as a yellow viscous oil. 88% yield; b.p.196-197°C (5 mmHg).

^{1}H NMR ($CDCl_3$, 400 MHz): δ 1.86-1.94 (quint, *J* = 7.4 Hz, 2H, -SCH_2-CH_2-), 2.61-2.68 (m, 4H, -S-CH_2-CH_2-CH_2-), 3.22 (s, 2H, -S-CH_2-$COOCH_3$), 3.71 (s, 3H, -CH_2COO-CH_3), 3.78 (s, 3H, ArOCH_2COO-CH_3), 3.87 (s, 3H, ArO-CH_3), 4.66 (s, 2H, ArO-CH_2-$COOCH_3$), 6.66-6.78 (m, 3H, Ar-*H*) ppm; ^{13}C NMR ($CDCl_3$, 100.6 MHz): δ 30.50 (-S-CH_2-$CH_2$$CH_2$-), 31.97 (-$SCH_2$-C$H_2$-$CH_2$-), 33.35 (-$SCH_2CH_2$-C$H_2$-), 34.16 (-S-C$H_2$-$COOCH_3$), 52.01 (-$SCH_2$COO-C$H_3$), 52.23 (Ar$OCH_2$COO-C$H_3$), 55.85 (ArO-C$H_3$), 66.67 (ArO-C$H_2$-$COOCH_3$), 112.57 (Ar-*C*), 114.74 (Ar-*C*), 120.28 (Ar-*C*), 135.82 (Ar-*C*), 145.52 (Ar-*C*), 149.58 (Ar-*C*), 169.54 (ArOCH_2-*C*O-OCH_3), 170.85 (-SCH_2-*C*O-OCH_3) ppm; FTIR: 2949, 1739 (C=O), 1760 (C=O), 1514, 1277, 1150, 1008, 767 cm^{-1}; HRMS (ESI) m/z calcd for $C_{16}H_{23}O_6NaS$ $[M+Na]^+$: 365.1035, found 365.1035.

Preparation of monomer M2: 1,4-bis{2-methoxy-4-[3-(2-methoxy-2-oxoethyl)]thiopropyl}phenoxy butane. Precursor **P1** (11.34 g, 42 mmol), 1,4-dibromobutane (4.36 g, 20 mmol), anhydrous K_2CO_3 (6.06 g, 44 mmol), KI (0.166 g, 1 mmol), and 150 mL anhydrous CH_3CN were added into a 250 mL three-necked round bottom flask equipped with a magneton (Scheme 1). The reaction mixture was refluxed at 82°C for 48 h in the protection of nitrogen. Then the suspension was cooled to room temperature, white solid was filtered off. The filtrate was concentrated under vacuum, then the residue viscous oil was dissolved in 200 mL dichloromethane, and successively washed by water (2 × 80 mL) and saturated NaCl solution (2 × 80 mL). The organic phase was dried over anhydrous magnesium sulphate, concentrated under vacuum. The resulting residue was immediately purified by twice-recrystallization from methanol to afford 9.74 g **M2** as a white crystalline solid. 86% yield; m.p.78-79°C.

^{1}H NMR ($CDCl_3$, 400 MHz): δ 1.87-1.94 (quint, *J* = 7.2 Hz, 4H, -SCH_2-CH_2-), 2.01 (m, 4H, -OCH_2-CH_2-), 2.62-2.67 (m, 8H, -S-CH_2-CH_2-CH_2-Ar), 3.22 (s, 4H, -S-CH_2-$COOCH_3$), 3.72 (s, 6H, -SCH_2COO-CH_3), 3.84 (s, 6H, ArO-CH_3), 4.06 (m, 4H, ArO-CH_2-), 6.67-6.82 (m, 3H, Ar-*H*) ppm; ^{13}C NMR ($CDCl_3$, 100.6 MHz): δ 26.10 (-OCH_2-CH_2-), 30.68 (-SCH_2-CH_2-CH_2Ar), 32.10 (-S-CH_2-CH_2CH_2Ar), 33.48 (-SCH_2CH_2-CH_2-Ar), 34.23 (-S-CH_2-$COOCH_3$), 52.33 (-SCH_2COO-CH_3), 56.00 (ArO-CH_3), 68.88 (ArO-CH_2-CH_2-), 112.45 (Ar-*C*), 113.48 (Ar-*C*), 120.41 (Ar-*C*), 134.14 (Ar-*C*), 146.83 (Ar-*C*), 149.47 (Ar-*C*), 170.96 (-SCH_2-*C*O-OCH_3) ppm; FTIR: 2956, 1730 (C=O), 1514, 1225, 1139, 1006, 781 cm^{-1}; HRMS (ESI) m/z calcd for $C_{30}H_{42}O_8NaS_2$ $[M+Na]^+$: 617.2219, found 617.2218.

General procedure for synthesis of polyesters

The polymerization reactions were performed in a 50 mL Schlenk flask equipped with a magneton, a nitrogen inlet and a vacuum distillation outlet (Scheme 2). Allowing for the low boiling points of short-chain α,ω-diols (n = 2, 3, 4, 6), an excess of diols to diester was needed to compensate the loss of diols due to the volatile at high temperature. Furthermore, in order to diminish the loss of short-chain α,ω-diols as much as possible and enhance the utilization rate of resources, a continuous overheating method was adopted across the transesterification stage. The detailed experiment strategies are illustrated in Table 1 and Table S1. By means of screening the different feed ratios of diester to diol at the given conditions, satisfactory molecular weights and polydispersities were acquired (Table 2). As for long-chain α,ω-diols (n = 10, 12), the feed ratio of 1 : 1 was enough to obtain the expected molecular weight. Tetrabutyl titanate (TBT, 0.6% mmol per mol of diester) was the choice of catalyst. The polymerization reactions were conducted with the frequently-used two-step melt polycondensation method with a vacuum of 0.03-0.06 mbar. Before transesterfication reaction, the apparatus was vented with nitrogen for 10 minutes in order to guarantee that there was no oxygen remaining in the system.

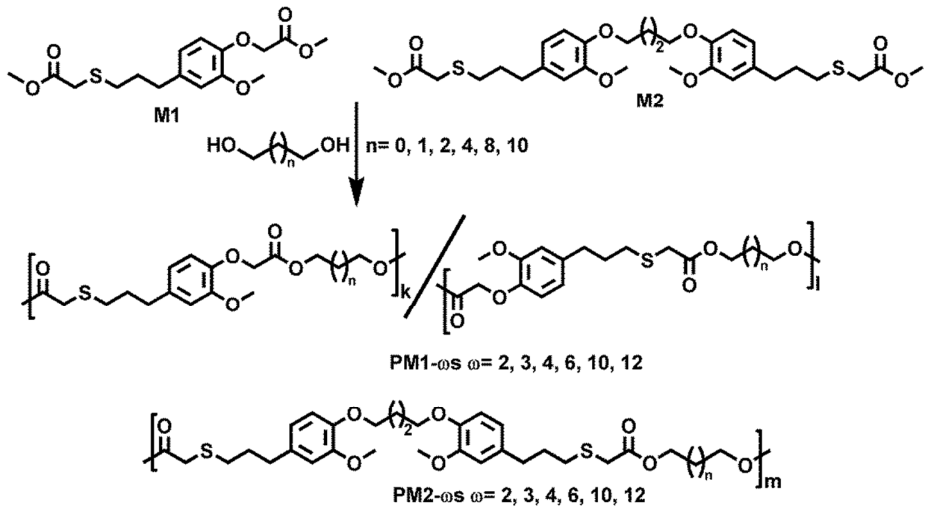

Scheme 2 synthetic routes for the preparation of **PM1-ωs** and **PM2-ωs**.

Table 1 Polymerization strategies for the synthesis of **PM1-ωs** with α,ω-diols

Reaction time (h) / α,ω-diols	Transesterification temperature (°C)						Polycondensation temperature (°C)		
	50	80	100	120	140	160	160	180	200
1,2-ethylene glycol	0.5	0.5	1	1	1	2	2	2	1
1,3-propanediol	0.5	0.5	1	1	1	2	2	2	1
1,4-butanediol	0.5	0.5	0.5	1	1	2	2	1	1
1,6-hexanediol	0.5	0.5	0.5	1	1	2	1	2	1
1,10-decanediol	0.5	0.5	0.5	1	1	2	1	2	1
1,12-dodecanediol	0.5	0.5	0.5	1	1	2	1	2	2

Table 2 Feed ratios, molecular weights, polydispersities and isolated yields of the synthesized polyesters

Polymer	Diol : diester (mol : mol)	M_n (g mol^{-1})	M_w (g mol^{-1})	PDI	Isolated Yield
PM1-2	2.8:1	10300	18500	1.8	78%
PM1-3	2.5:1	10800	20500	1.9	82%
PM1-4	1.8:1	20400	40000	1.9	84%
PM1-6	1.2:1	21800	39200	1.8	87%
PM1-10	1:1	45700	90500	1.9	88%
PM1-12	1:1	35800	65600	1.8	88%
PM2-2	2.8:1	13800	25900	1.8	75%
PM2-3	2.5:1	15200	32000	2.1	74%
PM2-4	1.8:1	12700	25000	1.9	78%
PM2-6	1.2:1	26000	53000	2.0	85%
PM2-10	1:1	39700	90100	2.2	89%
PM2-12	1:1	36100	69700	1.9	90%

Polycondensation stage was stopped until the stirrer was stuck, indicating the well proceeding of the reaction. Subsequently, the atmospheric pressure was recovered with nitrogen to prevent the degradation of the product until the reaction mixture was cooled to room temperature. The obtained polymers were dissolved in a minimum amount of chloroform and precipitated in excess methanol to remove the oligomers and impurities. Finally, the polymer was obtained as yellow viscous amorphous material by decanting the supernatant. The characterization data of **PM1-2** were presented as follows, and other obtained polymers have the similar affiliation and can be referred to their corresponding spectra (Fig. S8-S26).

PM1-2. ^{1}H NMR ($CDCl_3$, 400 MHz): δ 1.85-1.93 (quint, *J* = 7.4 Hz, 2H, -SCH_2-CH_2-CH_2-), 2.63-2.65 (m, 4H, -S-CH_2-CH_2-CH_2-), 3.21 (s, 2H, -S-CH_2-CO-), 3.85 (s, 3H, ArO-CH_3), 4.32-4.40 (m, 4H, -COO-CH_2-), 4.65-4.67 (s, 2H, ArO-CH_2-CO-), 6.65-6.78 (m, 3H, Ar-*H*) ppm; ^{13}C NMR ($CDCl_3$, 100.6 MHz): δ 30.42 (-SCH_2-CH_2-CH_2-), 31.85 (-S-CH_2-CH_2CH_2-), 33.15 (-SCH_2CH_2-CH_2-), 34.04 (-S-CH_2-CO-), 55.78 (ArO-CH_3), 62.47-62.65 (m, -COO-CH_2-), 66.34 (ArO-CH_2-CO-), 112.62 (Ar-*C*), 114.80 (Ar-*C*), 120.19 (Ar-*C*), 135.77 (Ar-*C*), 145.38 (Ar-*C*), 149.46 (Ar-*C*), 168.89 (ArOCH_2- *C*O-), 170.15 (-SCH_2-*C*O-) ppm; FTIR: 2925, 1758 (C=O), 1737 (C=O), 1513, 1270, 1147, 1035, 766 cm^{-1}.

Results and discussion

Synthesis of precursor and monomers

Precursor P1 derived from eugenol. Eugenol, as a naturally-occurring raw material, contains an allyl group and a phenolic hydroxyl group on the same aromatic ring. The distinctive structural characteristics make it easy to derivatize. Since the proposition of click reaction by Sharpless in 2001,[42] scientists have always devoted to explore novel types of click reactions. Radical-mediated thiol-ene coupling reaction, which has all the characteristics of click reactions, provides an appealing route to heteroatom-linked molecular systems.[44] Consequently S-linked ester group, hydroxyl or other functional groups can be introduced onto the substrates. The terminal olefinic group on

eugenol provides a perfect template for thiol-ene coupling reactions, hence can introduce an ester group on one side of eugenol. On the other side, the phenolic hydroxyl group can carry out nucleophilic substitution reactions. In this way, monomers with bifunctional ester groups can be successfully prepared. In this study, the expected precursor **P1** was obtained via one-step thiol-ene coupling reaction. For detailed, eugenol and methyl thioglycolate were initiated by DMPA under the UV radiation, and detected by TLC until the reactant eugenol disappeared, indicating the completion of the reaction. In the ^{1}H NMR spectrum of **P1** (Fig. S1), the appearance of two singlets at δ 3.22 and 3.72 ppm, as well as one quint at δ 1.85 to 1.93 ppm, and the disappearance of the characteristic peaks of the terminal olefinic protons at δ 4.93 and 5.79 ppm, indicate the formation of the thioether linkage in **P1**. The ^{13}C NMR spectrum (Fig. S2) and HRMS of **P1** also demonstrated that methyl thioglycolate was successfully linked to the eugenol.

Monomers M1 and M2 prepared from precursor P1. With the precursor **P1** in hand, monomers **M1** and **M2** were synthesized according to the commonly used nucleophilic substitution reactions. Firstly, precursor **P1** and methyl chloroacetate under K_2CO_3 and KI, acetonitrile as the solvent, were refluxed at 82°C for 6 h to give the desired monomer **M1** containing single aromatic ring with yield of 88%. In the ^{1}H NMR spectrum of **M1** (Fig. S3), the singlet peak at δ 4.66 ppm is assigned to the methylene protons adjacent to the phenoxy group, and the singlet peak at δ 3.79 ppm is attributed to the methyl protons of the methyl ester group introduced by methyl chloroacetate. Moreover, in order to obtain eugenol-based double aromatic ring containing diester monomer with tunable properties for comparation with **M1**, 1,4-dibromobutane bridged diester monomer **M2**, was prepared from the reaction of 2.1 equiv. of precursor **P1** with 1 equiv. of 1, 4-dibromobutane in CH_3CN. It has been reported that the incorporation of phenoxy ether linkages will increase the solubility, processability, and toughness of the aromatic polymers without any compromise of the thermal properties.[45] In the ^{1}H NMR spectrum of **M2** (Fig. S3), a singlet peak at δ 3.72 ppm is assigned to the two methyl protons of the methyl ester groups. The singlet peak at δ 4.07 ppm and the multiple peaks around 2.01 ppm are attributed to the methylene groups previously belonging to 1,4-dibromobutane. There are four irregularly splitting peaks between δ 6.68–6.82 ppm, which are assigned to the six protons on the two phenyl rings. The structures of **M1** and **M2** were also confirmed by ^{13}C NMR (Fig. S4, Fig. S5) and HRMS.

Synthesis of polyesters

The eugenol-based monomers **M1** and **M2** were polymerized with linear aliphatic α,ω-diols via a modified two-step melt polycondensation as shown in Scheme 2. In order to reduce the volatilization of α,ω-diols as much as possible and advocate the strategy of sustainable development, a continuous overheating method was adopted across the transesterification stage. That is, under the premise that the transesterification reactions proceeded efficiently, the selection of transesterification temperature should be as low as possible to diminish the loss of α,ω-diols as much as possible, especially for those short-chain α,ω-diols (n = 2, 3, 4, 6). Due to the catalytic activity of TBT is particularly related with the temperature, the transesterification reactions could be carried out well just when the reactions reached its activation energy.[46] In consequence, excessively low temperature was unfavourable to the transesterification reactions. For long-chain α,ω-diols (n = 10, 12), when the transesterification temperature was maintained below 120°C, the viscosity of the reaction system could not increase in spite of several hours. And when the reaction temperature was above 140°C, especially 160°C, the viscosity increased rapidly. This illustrates that temperature is crucial for the catalytic activity of TBT. For short-chain α,ω-diols (n = 2, 3, 4, 6), the degree of transesterification could not estimate from the viscosity of the reaction system due to the primarily created dihydroxyl alkyl esters of monomers during the transesterification, just like the industrial production process of PET or PBT.[47, 48] A compromise between the loss of α,ω-diols and catalytic activity of TBT was required to be made in order to choose the optimal transesterification temperature. In terms of short-chain aliphatic diol (n = 2, 3, 4, 6), an excess of diols to diesters was needed to compensate the loss of diols because of its lower boiling point. By means of optimizing the reaction conditions (time and temperature) and selecting the appropriate ratio of diol to diester, polyesters with satisfactory molecular weights and polydispersities were obtained. The detailed executive process was not presented. The data in Table 1 and Table S1 were the ultimate choice by means of screening the feed ratios, reaction temperatures and times. The optimal ratios of diol to diester for ethylene glycol, 1,3-propanediol, 1,4-butanediol, 1,6-hexanediol are 2.8:1, 2.5:1, 1.8:1 and 1.2:1, respectively (Table 2). Such feed ratios were also applied to **PM2-ωs**. For long-chain α,ω-diol (n = 10, 12), a ratio of 1:1 for diol to diester was sufficient to obtain the expected molecular weight. All obtained polymers are yellow viscous amorphous solids. The SEC traces (Fig. S6 and Fig. S7) and detailed analytical data of the obtained polymers are summarized in Table 2. In conclusion, the prepared polyesters have weight-average molecular weights in the 18500-90500 g mol^{-1} range, and polydispersities between 1.8 and 2.2. The huge discrepancy of M_w is largely ascribed to the uncontrolled stoichiometric feed ratios. It should be noted that in Table 2 the molecular weights and yields of polyesters increase with the molecular weights of diols. This is because that the stoichiometric ratio of diesters to diols has crucial influence on the molecular weight. Regarding short-chain diols (n = 2, 3, 4, 6), due to the volatilization of low-boiling diols, the stoichiometric ratios of diesters to diols are difficult to be strictly controlled to be 1:1. Therefore, very high molecular weight cannot be reached for short diols. However for long-chain diols (n = 10, 12), the higher boiling points make diols difficult to volatilize and hence the strict 1:1 stoichiometric ratios of diesters to diols could be maintained. Therefore, in

Table 2, the molecular weight of obtained polyesters increases with molecular weights of diols. In addition, the polyester is difficult to be dissolved in methanol during the post precipitations with the increase of molecular weight. Therefore, the polyesters prepared from long-chain diols showed higher yields.

The chemical structures of the obtained polyesters were characterized by ^{1}H NMR (Fig. S8-S11), ^{13}C NMR (Fig. S12-S23) and FTIR (Fig. S24-S26). All peaks in the spectra were easily assigned referring to the spectra of monomers. From the spectra of representative polyesters in Fig. S8 and Fig. S10, the corresponding chemical shifts have exclusively slight fluctuation with the changes of α,ω-diol length, which is due to the difference of chemical environment. For example, the singlet corresponding to the adjacent methylene of phenolic group altered from 4.66 ppm in **M1** to 4.57 ppm in **PM1-10**. Simultaneously, the downshift (from 3.22 to 3.13 ppm) of the methylene group introduced by methyl thioglycolate in **PM1-10** was also observed. More interestingly, the peaks corresponding to the two methylenes adjacent to hydroxyl of substrate α,ω-diols in the serials of **PM1-ωs** are split into two triplets, but not the situation in the serial of **PM2-ωs** (Fig. S8-S11). The reason for such difference is attributed to the unsymmetrical nature of **M1**, which bring about two types of ester groups with different chemical environment in **M1**. Meanwhile, **M2** is symmetrical resulting in just one type of ester groups with the same chemical environment. Either the two triplets between 4.02 and 4.39 ppm in **PM1-ωs** or the singlet between 4.08 and 4.12 ppm in **PM2-ωs** are gradually moved to the upfield with the increase of α,ω-diol length to the extent that they can hardly be separated from the peaks corresponding to the methylene adjacent to phenolic group in the ^{1}H NMR spectra of **PM2-ωs** (Fig. S10 and Fig. S11)**.** This can be explained by the electronic effect of α,ω-diol. The detailed discussion about chemical microstructures is presented in the following section. The difference of ester in **PM1-ωs** and **PM2-ωs** was also reflected in FTIR spectra. In the FTIR spectra of **PM1-ωs**, there are two ester carbonyl stretching vibrations at approximate 1731 and 1755 cm^{-1} (Fig. S24 and Fig. S25). Meanwhile, just one ester carbonyl stretching vibration at about 1731 cm^{-1} appears in the FTIR spectra of **PM2-ωs** (Fig. S25 and Fig. S26).

Chemical microstructure

The quantitative ^{13}C NMR spectroscopy was used to analyse the chemical microstructures of the synthesized polyesters. As shown in Fig. 1, the resonances of all magnetically different carbon atoms present in the backbone of the representative polyester **PM1-4** are obviously resolved taking profit from the sensitiveness of the methylene groups adjacent to hydroxyl functions of substrate 1,4-butanediol to sequence distributions at the dyad level. As mentioned above, this is resulted from the unsymmetry of ester functional groups in **M1**. The signals corresponding to those carbons split into four peaks ranging from 64.4 to 64.7 ppm since four types of dyads (***RR***, ***LL***, ***RL*** and ***LR***) are possible. However, the four peaks are not well resolved in all samples due to the difference of the two ester carbonyls' chemical environment are not enough to split the signals well. For **PM1-10** (Fig. S27), there are only two peaks between 64.2-64.6 ppm. The **PM1-ωs** exhibit completely randomness via integrating the areas of the four peaks roughly. That is, the orientations of **M1** that are incorporated into the polymer chains in an arbitrary manner. For **M2** containing two magnetically same ester carbonyl functions, it is certainly absent from this situation. The methylene groups adjacent to hydroxyl function will inevitably not split at the dyad level in the ^{13}C NMR spectra (Fig. S28). The negligible peaks at 62.44 ppm and 65.07, 64.78 ppm for **PM2-3** and **PM2-4**, respectively, are attributed to the terminal methylene groups along the polymer chains.

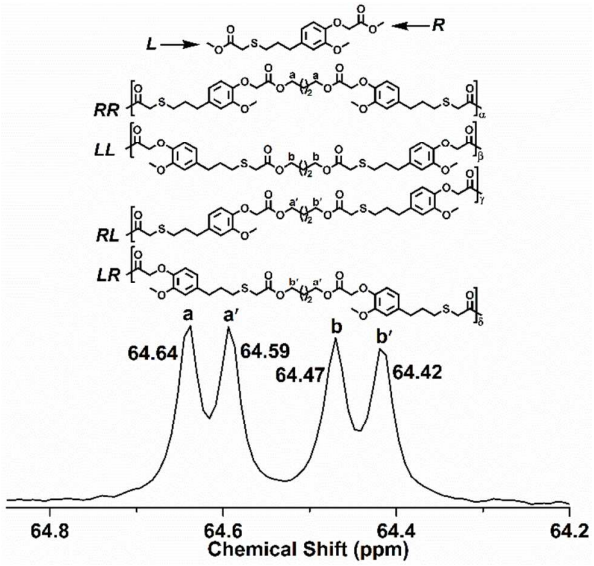

Fig. 1 ^{13}C NMR signals used for the microstructure analysis of the representative polyester **PM1-4** with schematic representation of dyads to which they are assigned.

Thermal Properties of the Polyesters

The thermal stability of the prepared polyesters was evaluated by TGA under a nitrogen atmosphere. TGA and TGA derivative curves of **PM1-ωs** and **PM2-ωs** measured from 25 to 600°C at a heating rate of 10 °C min^{-1} are shown in Fig. 2-3 and Fig. S29-S30. The thermal properties, *i.e*. temperatures at 5% weight loss and the maximal decomposition rate are outlined in Table 3, and the variation tendency of thermal property versus α,ω-diol length is present in Fig. 6. The two series of polyesters are thermally stable up to 339-365°C. Single-step narrow degradation curves are observed for all of them with maximum degradation rates in the range of 367-396°C. The stability increases gradually with the length of α,ω-diol as for **PM1-ωs**, while the case of **PM2-ωs** is a little obscure. In other words, the stability of **PM2-ωs** with short-chain α,ω-diol (ω = 2, 3, 4) gradually decreases with the length of α,ω-diol, but the stability of **PM2-ωs** with long-chain α,ω-diol (ω = 6, 10, 12) gradually increased with the length of α,ω-diol. The maximum degradation rate also complies with the same rules as thermal stability with respect to **PM1-ωs**. The maximum degradation rate increased with the length of the aliphatic α,ω-diol. For **PM2-ωs**,

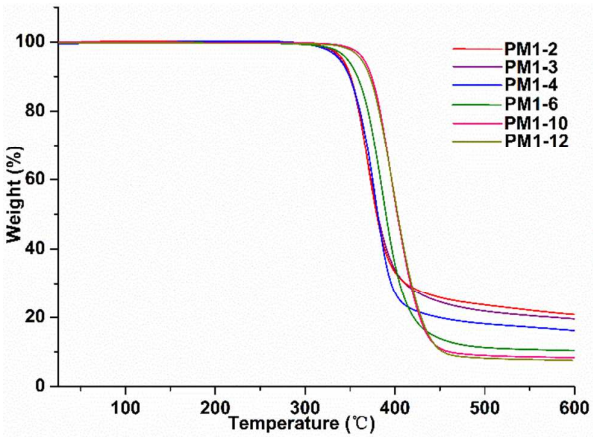

Fig. 2 TGA traces of **PM1-ωs** recorded from 25-600°C at a heating rate of 10 °C min^{-1} under a nitrogen atmosphere.

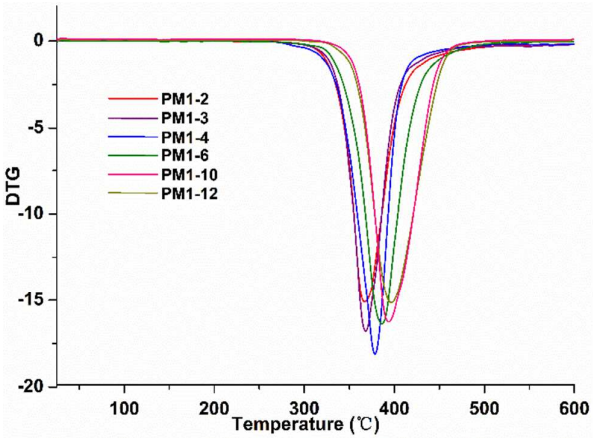

Fig. 3 TGA derivative traces of **PM1-ωs** recorded from 25-600°C at 10 °C min^{-1} under a nitrogen atmosphere.

Table 3 Thermal properties of **PM1-ωs** and **PM2-ωs** obtained by TGA and DSC analysis

Polymer	T_g [a] (°C)	$T_{5\%}$ [b] (°C)	T_d [c] (°C)	W [d] (%)
PM1-2	7.6	339	367	19.56
PM1-3	-3.6	341	368	20.78
PM1-4	-8.2	339	378	16.7
PM1-6	-16.5	346	386	10.3
PM1-10	-27.6	365	393	8.2
PM1-12	-28.4	363	396	7.8
PM2-2	-3.7	356	383	15.5
PM2-3	-7.3	359	389	17.1
PM2-4	-9.7	349	393	11.6
PM2-6	-12.2	345	377	15.0
PM2-10	-17.3	347	381	13.1
PM2-12	-22.2	362	391	9.5

[a] Glass transition temperature measured in DSC during the -2nd heating scan at 10°C min^{-1}. [b] Temperature at which 5% weight loss was observed. [c] Temperature for maximum degradation rate. [d] Remaining weight at 600 °C.

their maximum degradation rate complied with another rule. Polyesters prepared from both short-chain α,ω-diols (ω = 2, 3, 4) and long-chain α,ω-diols (ω = 6, 10, 12), exhibit an increasing tendency of their maximum degradation rates. In general, polyesters bearing short-chain α,ω-diols (ω = 2, 3, 4) show superior maximum degradation rates than polyesters bearing long-chain α,ω-diols (ω = 6, 10, 12). The remaining residual weights at 600°C are located in the range of 7.8%-20.7%. Linear aliphatic sections are known to decompose almost completely compared with aromatic sections under the same TGA conditions.[49] Both polyesters prepared from **M1** and **M2** with long-chain α,ω-diols have relatively higher proportions of aliphatic sections, resulting that the remaining weight gradually decreases with the length of the α,ω-diols. Compared **PM1-ωs** with **PM2-ωs**, the remaining weights of **PM1-ωs** are higher than **PM2-ωs** when short-chain α,ω-diols (ω = 2, 3, 4) are incorporated into the polyester chains. When 1,4-dibromobutane bridged **M2** is polymerized with short-chain α,ω-diol (ω = 2, 3, 4), the four methylenes originating from 1,4-dibromobutane act as a "diluent". Consequently, **PM2-ωs** (ω = 2, 3, 4) have higher proportions of aliphatic section. And when **M2** is polymerized with long-chain α,ω-diol (ω = 6, 10, 12), the four methylenes on the contrary act as a "densifier". Therefore, a high proportion of aromatic section means high residual weights.

The T_gs and other thermal behaviours of the polyesters were also studied by DSC at a 10°C min^{-1} heating and cooling rate. The second heating DSC curves measured from -80-150°C are

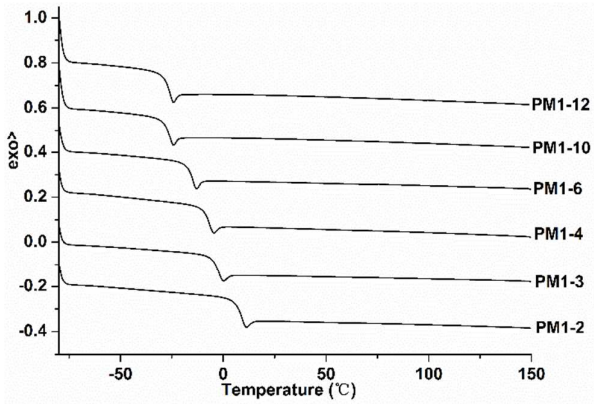

Fig. 4 second heating DSC curves of **PM1-ωs** carried out from -80 to 150°C at a heating /cooling rate of 10°C min^{-1}.

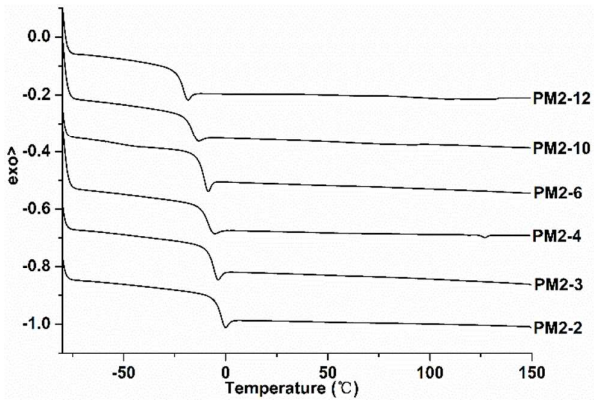

Fig. 5 second heating DSC curves of **PM2-ωs** carried out from -80 to 150°C at a heating /cooling rate of 10°C min^{-1}.

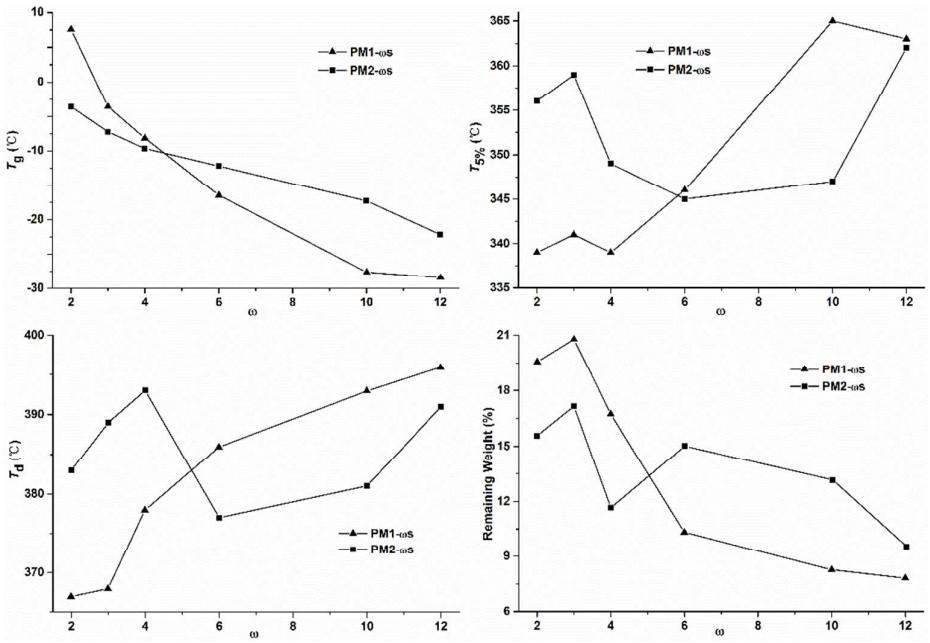

Fig. 6 the variation tendencies of T_gs, $T_{5\%}$, T_d and remaining weights versus ω.

shown in Fig. 4 and Fig. 5, and the corresponding thermal data are summarized in Table 3. As observed from DSC curves, the polyesters are predominantly amorphous materials due to the amorphism of **M1** and **M2**. The existence of methoxy group adjacent benzene ring in **M1** and **M2** impede the structural symmetry seriously, even though the incorporation of long-chain linear aliphatic α,ω-diols into the chains of polyesters cannot compensate the structural defection. On the contrary, the T_g steadily decreases with the increase of the number of methylene units in the diol segment. This is attributed to that the internal rotation along the main chains of polyesters becomes more favourable with the increasing of the α,ω-diol length. Random polymers derived from renewable eugenol seem to be more unfavourable for a regular crystal chains packing.

More interestingly, the T_gs of polyesters in **PM1-ωs** are higher than the corresponding polyesters in **PM2-ωs** when the number of methylene units in the diol is below 4. As illustrated in Table 3, the T_g of **PM1-2** (7.6°C) is obviously higher than that of **PM2-2** (-3.7°C). Whereas, when the numbers of methylene units in the diols are more than 4, the results are completely opposite. For instance, the T_g of **PM1-10** (-27.6°C) is obviously lower than that of **PM2-10** (-17.3°C). This phenomenon can be illustrated as follows. The density of rigid aromatic ring has a vital influence on the T_g. As we all know, aromatic ring is adverse to the internal rotation of the main polymer chains. When 1,4-dibromobutane bridged **M2** is polymerized with α,ω-diol (n≤4), the main chains of polyesters have less discrete aromatic rings than **M1**. Therefore, they are more flexible than that of **PM1-ωs** (n≤4). However, when the number of methylene in α,ω-diol is more than 4, the four aliphatic methylenes in **M2** is shorter than α,ω-diols. Therefore, the α,ω-diol here acts as a "diluent" for **PM2-ωs** (ω≥6). More methylenes in α,ω-diol, more obvious decrease of the T_g.

Stress-strain behaviour

A preliminary evaluation of the mechanical properties of the synthesized polyesters has been carried out by tensile test from casting films in chloroform. Owing to the no-crystallinity caused by the lack of symmetry, and the lower T_gs (-28.4 to 7.6°C, *i.e.* -28.4°C for **PM1-12**), which is nearly six dozens of centigrade below room temperature, the majority of polyesters exhibits unmanageable amorphous viscous solid. Just **PM1-4**, **PM1-10**, **PM2-4** and **PM2-10** could be casted into fashioned films to the best of our efforts. The stress-strain curves recorded from the essayed polyesters are presented in Fig. 7 and the mechanical parameters measured are accessible in Table 4. Apparently, the essayed polyesters show extremely superior viscosity property accompanying with inferior yield strength and ultimate strength. It is also in accordance with our previous expectation that **PM2-4** and **PM2-10** prepared from 1,4-dibromobutane bridged monomer **M2** exhibit superior toughness than **PM1-4** and **PM1-10** prepared from **M1** with single aromatic ring. The elongation at break reaches up to 840-1000% even in the action of smaller force, indicating the excellent viscosity of the materials. Polyester molecules emerge as the crimp state under natural conditions, and polymer chains can stretch along the direction of force due to the high flexibility of molecular chains. In terms of all the four polyesters (**PM1-4**, **PM1-10**, **PM2-4** and **PM2-10**), they start from yield point through an extraordinary long range of cold drawing, and finally enter into stress hardening, indicating the difficult orientation of macromolecular chains. As for eugenol-based polyesters containing short-chain α,ω-diols (1,4-butandiol), the structural asymmetry seems more observably for orientation than long-chain α,ω-diols (1,10-decanediol). The Young's modulus was observed to increase with the density of

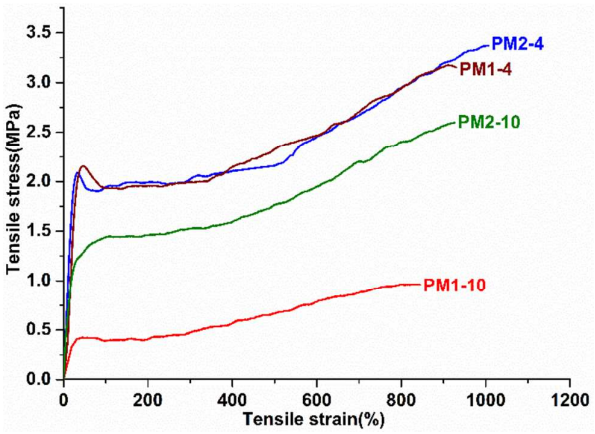

Fig. 7 Stress–strain curves of **PM1-4**, **PM1-10**, **PM2-4** and **PM2-10** at 50 mm min^{-1}.

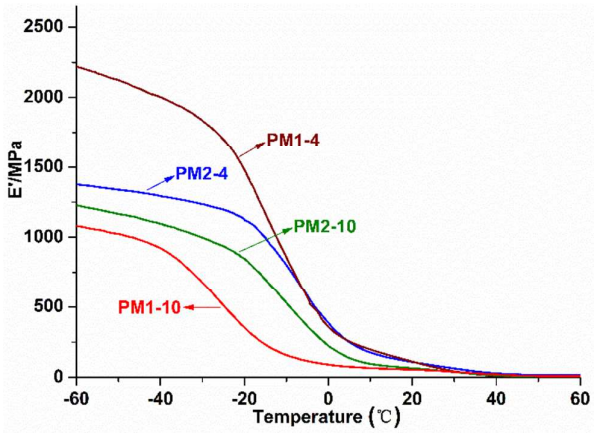

Fig. 8 Storage modulus as a function of temperature for **PM1-4**, **PM2-4**, **PM1-10** and **PM2-10**.

Table 4 Tensile parameters of the testing samples

Polymer	Young's modulus (MPa)	Ultimate strength (MPa)	Elongation at break (%)
PM1-4	5.1 ± 0.5	3.2 ± 0.5	930 ± 42
PM2-4	6.9 ± 0.8	3.4 ± 0.6	1006 ± 50
PM1-10	1.2 ± 0.6	1.0 ± 0.2	844 ± 35
PM2-10	4.0 ± 0.8	2.6 ± 0.3	926 ± 40
PET	1032 ± 52	45 ± 7	23 ± 5
PBT	863 ± 25	33 ± 4	15 ± 4

rigid benzene rings as it did the elongation at break and ultimate strength. Unfortunately, the values of Young's modulus are not high enough for the use as structural materials compared with conventional commercial PET (M_w : 32100, PDI : 2.5)[50] and PBT (M_w : 41500, PDI : 2.4),[48] the data of PET and PBT here are original. The presence of methoxy group adjacent to the phenolic hydroxyl of eugenol obviously reduces the structural symmetry and crystallinity so that the mechanical behavior of the polyesters is appreciably impaired as far as the whole range length of α,ω-diols is considered. More interestingly, as shown in Table 4, PET and PBT possess higher modulus and strengths, on the contrary the elongations at break are just 5-8%. The excellent ductility and viscosity of the two series of eugenol-based polyesters may be used as the toughening compensatory component of PET or PBT by copolymerization. It is well known that PET or PBT are brittle materials under generally conditions. Plasticizers are usually needed to add into the raw PET or PBT materials to improvetheir toughness and impact strength to reach the standard of structural materials.[51] Hence, copolymerization with the monomers derived from renewable eugenol may be a new idea to toughen PET and PBT. Furthermore, substitution or part substitution of fossil resources by renewable resources is also in accordance with the idea of green chemistry.

Dynamic mechanical analysis

Polymers, as structural materials, are often suffered from alternating stresses or alternating strains in practical applications. For example, tires, driving belts and gears all work in such situations. The study of strain or stress of materials versus time under alternating forces or strains is very necessary. In order to evaluate the dynamic viscoelasticity of

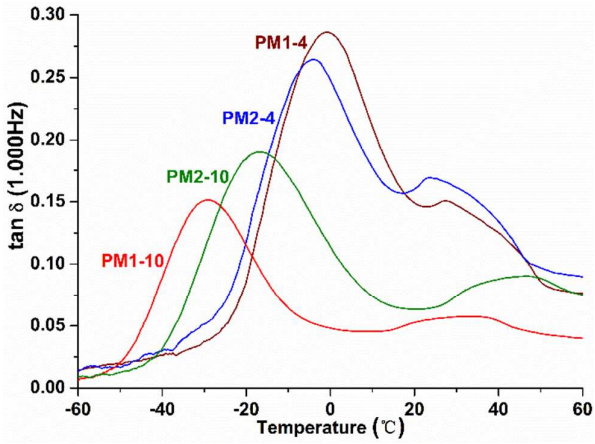

Fig. 9 tan δ as a function of temperature for **PM1-4**, **PM2-4**, **PM1-10** and **PM2-10**.

Table 5 Dynamic mechanical properties of **PM1-2**, **PM1-4**, **PM2-2** and **PM2-4**

Polymer	T_g(°C)	E'(20°C) (MPa)	tan δ_{max}
PM1-4	-5.23	124.70	0.28
PM2-4	-6.50	110.77	0.26
PM1-10	-30.31	52.54	0.15
PM2-10	-20.68	69.17	0.18

the synthesized polyesters, DMA were performed using a TA DMA 2928 in the controlled force-tension film mode in the -60 to 60°C range and at a heating rate of 3°C min^{-1}. Fig. 8 and Fig. 9 show the curves of the storage modulus (E′) and tan δ as a function of temperature, respectively. E′ represents the elastic storage energy when the materials are suffered from once alternating force. Owing to the hysteresis of the strain relative to the stress, a part of elastic storage energy always cannot be enough released. This part of energy is consumed on the friction of segment motion. The significantly drop of storage modulus around the T_g indicates that the hysteresis loss of the polyesters is very serious. This is inevitably because that the frozen segments begin to motion around the T_g, and that the structure of macromolecular chains has a crucial influence on the internal friction. As for polyesters containing high density of rigid aromatic benzene rings, *i.e.* **PM1-4** and **PM2-4**, the

internal friction is greater than **PM1-10** and **PM2-10**. Therefore, remarkable decrease of storage modulus was observed in Fig. 8. When the temperature was below the T_g, the majority of strain stemmed from the changes of the bond distances and the bond angles. The rate of strain was so quickly that there was not enough time for the motion of chain segments. Hence, the tan δ was not apparent. When temperature reached T_g, the frozen chain segment started to motion. Due to the high viscosity of the system, the internal friction resistance was also relevantly higher. The motion of segment chains became considerable troublesome resulting in delaying of strain to stress. As a result, obvious hysteresis loss peak was observed. The temperature at tan δ_{max} is in general regarded as the T_g. **PM1-4** and **PM2-4** containing short-chains α,ω-diols have higher aromatic ring density than **PM1-10** and **PM2-10**. In a consequence, **PM1-4** and **PM2-4** have higher internal friction resistance and induced higher hysteresis loss. As shown in Table 5, the tan δ_{max} are found to be rather higher. Consequently, such materials can absorb much impact energy or act as the toughening component, which are in accordance with the results obtained from the previous tensile test section.

Conclusions

In conclusion, high-purity DMT-like aromatic monomers derived from renewable eugenol were synthesized via the thiol-ene click reaction and the following nucleophilic substitution reactions. Two series of thermoplastics polyesters were prepared with linear aliphatic α,ω-diols via a continuous overheating method across the transesterification stage. By means of optimizing the reaction conditions (time, temperature and feed ratios), polyesters with satisfactory molecular weights and polydispersities were obtained. They all exhibit thermal stability above 330°C, and more importantly, the thermal stability, maximum degradation rate and residual weight at 600°C are intimately associated with the length of the linear aliphatic α,ω-diol. The synthesized polyesters are all amorphous materials due to the amorphism of **M1** and **M2** with glass transition temperatures ranging from -28.39 to 7.58°C. The length of α,ω-diol has also crucial influence on the T_g. With the gradually increase of the α,ω-diol length, the T_gs of either **PM1-ωs** or **PM2-ωs** uniformly exhibit a tendency of decreasing. Although the Young's modulus and ultimate strength are not relatively high, the ductility of eugenol-based polyesters is excellent, whose elongations at break reach up to 840-1000%. Consequently, PET or PBT may be toughened by copolymerization with the monomers derived from renewable eugenol. Eugenol-based polyesters may have potential applications on high impact materials.

Acknowlegement

This work was funded by NSFC (51203079), the Natural Science Foundation of Tianjin (14JCYBJC18100), and PCSIRT (IRT1257).

References

1. A. Corma, S. Iborra and A. Velty, *Chemical Reviews*, 2007, **107**, 2411-2502.
2. P. Gallezot, *Chemical Society Reviews*, 2012, **41**, 1538-1558.
3. C. H. Christensen, J. Rass-Hansen, C. C. Marsden, E. Taarning and K. Egeblad, *Chemsuschem*, 2008, **1**, 283-289.
4. R. A. Sheldon, *Green Chemistry*, 2014, **16**, 950-963.
5. S. Munoz-Guerra, C. Lavilla, C. Japu and A. M. de Ilarduya, *Green Chemistry*, 2014, **16**, 1716-1739.
6. M. G. Garcia-Martin, R. R. Perez, E. B. Hernandez, J. L. Espartero, S. Munoz-Guerra and J. A. Galbis, *Macromolecules*, 2005, **38**, 8664-8670.
7. G. Q. Chen and M. K. Patel, *Chemical Reviews*, 2012, **112**, 2082-2099.
8. B. Kamm, *Angewandte Chemie-International Edition*, 2007, **46**, 5056-5058.
9. P. N. R. Vennestrom, C. M. Osmundsen, C. H. Christensen and E. Taarning, *Angewandte Chemie-International Edition*, 2011, **50**, 10502-10509.
10. D. Dakshinamoorthy, S. P. Lewis, M. P. Cavazza, A. M. Hoover, D. F. Iwig, K. Damodaran and R. T. Mathers, *Green Chemistry*, 2014, **16**, 1774-1783.
11. D. J. Liu and E. Y. X. Chen, *Green Chemistry*, 2014, **16**, 964-981.
12. A. Behr, A. J. Vorholt, K. A. Ostrowski and T. Seidensticker, *Green Chemistry*, 2014, **16**, 982-1006.
13. A. Gandini, *Green Chemistry*, 2011, **13**, 1061-1083.
14. U. Biermann, W. Friedt, S. Lang, W. Luhs, G. Machmuller, J. O. Metzger, M. R. Klaas, H. J. Schafer and M. P. Schneider, *Angewandte Chemie-International Edition*, 2000, **39**, 2206-2224.
15. U. Biermann, U. Bornscheuer, M. A. R. Meier, J. O. Metzger and H. J. Schafer, *Angewandte Chemie-International Edition*, 2011, **50**, 3854-3871.
16. M. A. R. Meier, J. O. Metzger and U. S. Schubert, *Chemical Society Reviews*, 2007, **36**, 1788-1802.
17. J. Zakzeski, P. C. A. Bruijnincx, A. L. Jongerius and B. M. Weckhuysen, *Chemical Reviews*, 2010, **110**, 3552-3599.
18. H. Kobayashi and A. Fukuoka, *Green Chemistry*, 2013, **15**, 1740-1763.
19. F. Fenouillot, A. Rousseau, G. Colomines, R. Saint-Loup and J. P. Pascault, *Progress in Polymer Science*, 2010, **35**, 578-622.
20. A. F. Sousa, A. Gandini, A. J. D. Silvestre and C. P. Neto, *Chemsuschem*, 2008, **1**, 1020-1025.
21. J. A. Heredia-Guerrero, A. Heredia, R. Garcia-Segura and J. J. Benitez, *Polymer*, 2009, **50**, 5633-5637.
22. A. Gandini, D. Coelho, M. Gomes, B. Reis and A. Silvestre, *Journal of Materials Chemistry*, 2009, **19**, 8656-8664.
23. X. Q. Liu, W. B. Xin and J. W. Zhang, *Green Chemistry*, 2009, **11**, 1018-1025.
24. M. Bahr, A. Bitto and R. Mulhaupt, *Green Chemistry*, 2012, **14**, 1447-1454.

25. M. Firdaus, L. M. de Espinosa and M. A. R. Meier, *Macromolecules*, 2011, **44**, 7253-7262.
26. J. R. Lowe, M. T. Martello, W. B. Tolman and M. A. Hillmyer, *Polymer Chemistry*, 2011, **2**, 702-708.
27. P. Foley, A. K. Pour, E. S. Beach and J. B. Zimmerman, *Chemical Society Reviews*, 2012, **41**, 1499-1518.
28. R. Garces, E. Martinez-Force and J. J. Sales, *Grasas Y Aceites*, 2011, **62**, 21-28.
29. P. Malinowska, A. Gliszczynska-Swiglo and H. Szymusiak, *European Journal of Lipid Science and Technology*, 2014, **116**, 1553-1562.
30. T. Lebarbe, M. Neqal, E. Grau, C. Alfos and H. Cramail, *Green Chemistry*, 2014, **16**, 1755-1758.
31. D. Quinzler and S. Mecking, *Angewandte Chemie-International Edition*, 2010, **49**, 4306-4308.
32. M. Desroches, S. Caillol, V. Lapinte, R. Auvergne and B. Boutevin, *Macromolecules*, 2011, **44**, 2489-2500.
33. M. Winkler and M. A. R. Meier, *Green Chemistry*, 2014, **16**, 1784-1788.
34. R. Auvergne, S. Caillol, G. David, B. Boutevin and J. P. Pascault, *Chemical Reviews*, 2014, **114**, 1082-1115.
35. G. Lligadas, J. C. Ronda, M. Galia and V. Cadiz, *Biomacromolecules*, 2010, **11**, 2825-2835.
36. A. G. Pemba, J. A. Flores and S. A. Miller, *Green Chemistry*, 2013, **15**, 325-329.
37. O. Turunc, M. Firdaus, G. Klein and M. A. R. Meier, *Green Chemistry*, 2012, **14**, 2577-2583.
38. C. C. Pang, J. Zhang, G. L. Wu, Y. N. Wang, H. Gao and J. B. Ma, *Polymer Chemistry*, 2014, **5**, 2843-2853.
39. J. A. M. Lummiss, K. C. Oliveira, A. M. T. Pranckevicius, A. G. Santos, E. N. dos Santos and D. E. Fogg, *Journal of the American Chemical Society*, 2012, **134**, 18889-18891.
40. Q. Song, F. Wang and J. Xu, *Chemical Communications*, 2012, **48**, 7019-7021.
41. C. E. Hoyle, A. B. Lowe and C. N. Bowman, *Chemical Society Reviews*, 2010, **39**, 1355-1387.
42. H. C. Kolb, M. G. Finn and K. B. Sharpless, *Angewandte Chemie-International Edition*, 2001, **40**, 2004-2021.
43. E. Fuhrmann and J. Talbiersky, *Organic Process Research & Development*, 2005, **9**, 206-211.
44. C. E. Hoyle and C. N. Bowman, *Angewandte Chemie-International Edition*, 2010, **49**, 1540-1573.
45. G. P. Yu, C. Liu, J. Y. Wang, T. S. Gu and X. G. Jian, *Polymer Degradation and Stability*, 2009, **94**, 1053-1060.
46. L. Finelli, C. Lorenzetti, M. Messori, L. Sisti and M. Vannini, *Journal of Applied Polymer Science*, 2004, **92**, 1887-1892.
47. G. Z. Papageorgiou, V. Tsanaktsis and D. N. Bikiaris, *Physical Chemistry Chemical Physics*, 2014, **16**, 7946-7958.
48. C. Japu, A. M. de Ilarduya, A. Alla, M. G. Garcia-Martin, J. A. Galbis and S. Munoz-Guerra, *Polymer Chemistry*, 2014, **5**, 3190-3202.
49. J. Wu, P. Eduard, L. Jasinska-Walc, A. Rozanski, B. A. J. Noordover, D. S. van Es and C. E. Koning, *Macromolecules*, 2013, **46**, 384-394.
50. C. Japu, A. M. de Ilarduya, A. Alla, M. G. Garcia-Martin, J. A. Galbis and S. Munoz-Guerra, *Polymer Chemistry*, 2013, **4**, 3524-3536.
51. L. M. de Espinosa, A. Gevers, B. Woldt, M. Grass and M. A. R. Meier, *Green Chemistry*, 2014, **16**, 1883-1896.

Entry for the Table of Contents

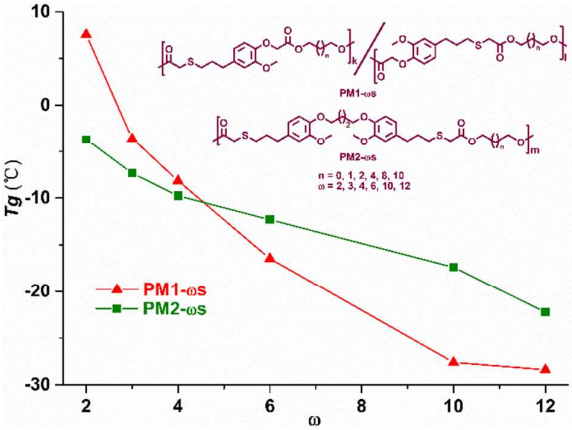

Two series of thermoplastic polyesters derived from renewable eugenol and linear aliphatic α,ω-diols were prepared: the dependence of property versus α,ω-diol length